Color appearance of spatial patterns compared by direct estimation and conjoint measurement

Frédéric Devinck, Kenneth Knoblauch

Color appearance of spatial patterns compared by direct estimation and conjoint measurement

FRÉDÉRIC DEVINCK,[1,*] AND KENNETH KNOBLAUCH[2,3,4]

[1]*Université Rennes 2, LP3C, EA 1285, 35000 Rennes, France*
[2]*INSERM U1208 Stem-Cell and Brain Research Institute, Department of Integrative Neurosciences, 69675 Bron Cedex, France*
[3]*Université Lyon 1, 69003 Lyon, France*
[4]*National Centre for Optics, Vision and Eye Care, Faculty of Health and Social Sciences, University of South-Eastern Norway, Kongsberg, Norway*
**Frederic.devinck@univ-rennes2.fr*

Abstract: Perceptual scales of color saturation as obtained by direct estimation (DE) and maximum likelihood conjoint measurement (MLCM) were compared for red checkerboard patterns and uniform red squares. For the direct estimation task, observers were asked to rate the saturation level as a percentage, indicating the chromatic sensation for each pattern and contrast. For the MLCM procedure, observers judged on each trial which of two stimuli that varied in chromatic contrast and/or spatial pattern evoked the most salient color. In separate experiments, patterns varying only in luminance contrast were also tested. The MLCM data confirmed previous results reported with DE indicating that the slope of the checkerboard scale with cone contrast levels is steeper than that for the uniform square. Similar results were obtained with patterns modulated only in luminance. DE methods were relatively more variable within observer, reflecting observer uncertainty, while MLCM scales showed greater relative variability across observers, perhaps reflecting individual differences in the appearance of the stimuli. MLCM provides a reliable scaling method, based only on ordinal judgments between pairs of stimuli and that provides less opportunity for subject-specific biases and strategies to intervene in perceptual judgements.

1. Introduction

Direct estimation (DE) is commonly used in color vision studies to measure hue and saturation perception [1,2]. While the method has been carefully validated [3], it has been criticized as being nonintuitive for naïve observers, subject to cultural or linguistic biases and dependent on an observer's capacity to translate percepts into numbers [4]. A recent study sought to address these criticisms by using a similarity rather than a rating procedure [4].

Over the last 20 years, scaling methods have been introduced that are based on simple ordinal comparisons of stimuli, and the perceptual scales are estimated to maximize the likelihood of the observer's judgments over the experimental trials within the framework of a signal detection model of the decision process [5-7]. Ordinal comparisons would be expected to be easier to make than subjective ratings, and these methods offer a more rigorous procedure for obtaining scale values. Nevertheless, there are no guarantees that both methods would generate the same results. Here, we compare DE and Maximum Likelihood Conjoint Measurement (MLCM) in a replication of experiments that investigated the influence of spatial complexity and cone contrast on color appearance. MLCM is based on paired-comparisons and is used to estimate perceptual scales associated with the integration of information along multiple dimensions [8-10].

Recently, Shapley, Nunez & Gordon (2019) argued that two separate systems contribute to color appearance [11]. One system is sensitive to low chromatic contrasts and responds best to low spatial frequencies while the other is most active at high chromatic contrasts and has a band-pass frequency characteristic. This hypothesis is based on the neural responses of two color-sensitive cell classes described in primate cortical area V1: single-opponent and double-opponent cells [12-18]. Single-opponent cells respond best to the low spatial frequency content of chromatic patterns (< 0.5 c/deg) and display a fall-off in sensitivity to high frequency chromatic patterns. In contrast, double-opponent cells display a band-pass sensitivity, with greater selectivity for patterns at higher spatial frequencies (2 c/deg) with response fall-off to patterns at both low and high spatial frequencies [12,17,19].

Nunez, Shapley & Gordon (2018) used a direct estimation (DE) [20], saturation scaling method to estimate the appearances of equiluminant uniform and high frequency checkerboard stimuli under the assumption that these stimuli would preferentially activate single- or double-opponent cell classes, respectively. The perceived saturation of both stimuli increased as a function of cone contrast, but the checkerboard pattern increased more steeply than the uniform square field for the equivalent size and cone contrasts. Thus, the strength of the estimated color appearance was stronger for stimuli designed to preferentially activate double-opponent rather than single-opponent cell classes. These results were supported by VEP measurements which provided evidence for two different mechanisms underlying the responses to the two patterns [20,21].

Here, we replicate the DE procedure of Nunez et al. (2018) for reddish equiluminant stimuli and compare the results with those obtained using MLCM. We also compared the methods using patterns varying only in luminance.

2. General Methods

2.1 Observers

Seven observers participated in the experiments, six of whom were naïve to the purpose of the study. Ages ranged from 26 to 46 years. All observers had normal color vision as tested by a Farnsworth Panel D15 and had normal or corrected-to-normal visual acuity. We tested five participants for each task. The same five observers participated in the DE and the MLCM tasks for patterns displayed along a given axis. For the MCLM and the direct estimation tasks with patterns displayed along the L+M axis, three observers from the previous tasks remained, and two additional participants were recruited. All studies were conducted in agreement with the Declaration of Helsinki for the protection of human subjects.

2.2 Apparatus

The experiments were run in a dark room and were programmed using MATLAB 7.9 (MathWorks, http://mathworks.com) and the CRS Toolbox. The stimuli were presented on a NEC MultiSync FP2141sb color CRT monitor driven by a Cambridge Research ViSaGe graphic board with a color resolution of 14 bits per gun (Cambridge Research Systems, Rochester, United Kingdom). The monitor had a diagonal screen size of 22 inches, resolution of 1024 × 768 pixels, and a refresh rate of 120 Hz. The screen was calibrated using a SpectroCal spectroradiometer with the calibration routines of Cambridge Research Systems. A Cedrus RB540 response pad was used to collect observer responses (Cedrus Corporation; San Pedro, CA, USA). Observer position was stabilized by a chinrest so that the screen was viewed binocularly at a distance of 80 cm.

2.3 Stimuli

Observers viewed a red-gray checkerboard pattern, or a red square displayed on a gray background. In a separate session, a white-gray checkerboard pattern and a white square were also used. The same spatial patterns were used for the DE method and the MLCM procedure though more contrast levels were tested using MLCM. Stimuli were designed to be similar to those used by Nunez et al. [20,21,29].

The stimulus size measured 10 × 10 deg. The checkerboard had 32 × 32 checks, each of dimensions 0.3141 × 0.3141 deg. The choice of the checkerboard and square sizes were chosen according to the values used by Nunez et al. (2018). As they did, all stimuli were vignetted by a stationary Gaussian window (σ = 2 deg). Thus, the checkerboard and the square faded gradually to the background gray color moving away from the stimulus center. The gray background had fixed chromatic coordinates (x,y = 0.30, 0.35; Y = 29.89 cd/m^2), whereas 6 and 10 different chromatic values were used for the DE and for the MLCM procedures, respectively. The CIE coordinates are provided in Table I (red stimuli) and II (white stimuli). Note that for the red stimuli, contrast values differed from those used by Nunez et al. (2018) but these values overlapped extensively. For the luminance conditions, values ranged from 36.16 cd/m^2 to 111.60 cd/m^2.

Table 1. CIE color coordinates, cone contrast (the difference between the cone excitation of the stimulus and the cone excitation of background divided by the cone excitation of the background) and the contrast measured for each red color presented.

MLCM	CIE coordinates			Cone values			Contrast
	x	y	Y	L	M	S	$\frac{\sqrt{\left(\frac{\Delta L}{L}\right)^2+\left(\frac{\Delta M}{M}\right)^2+\left(\frac{\Delta S}{S}\right)^2}}{\sqrt{3}}$
	0.3147	0.3440	30.36	19.9356	10.5941	0.2281	0.0189
	0.3290	0.3391	30.72	20.4461	10.4459	0.2279	0.0356
	0.3420	0.3325	31	20.9114	10.2650	0.2302	0.0531
	0.3421	0.3228	31.04	21.0366	10.1923	0.2445	0.0739
	0.3720	0.3229	32.14	22.3234	9.9991	0.2308	0.0971
	0.3848	0.3178	32.82	23.1016	9.9059	0.2336	0.1213
	0.3992	0.3141	33.86	24.1695	9.8825	0.2354	0.1521
	0.4121	0.3103	34.75	25.1287	9.8176	0.2370	0.1809
	0.4240	0.3087	36.1	26.3870	9.9134	0.2385	0.2164
	0.4369	0.3065	37.9	28.0368	10.0701	0.2424	0.2645
Direct Estimation	x	y	Y	L	M	S	$\frac{\sqrt{\left(\frac{\Delta L}{L}\right)^2+\left(\frac{\Delta M}{M}\right)^2+\left(\frac{\Delta S}{S}\right)^2}}{\sqrt{3}}$
	0.3147	0.3440	30.36	19.9356	10.5941	0.2281	0.0189
	0.34	0.33	30.62	20.6199	10.1729	0.2260	0.0473
	0.37	0.32	31.6	21.8173	9.9622	0.2286	0.0838
	0.39	0.32	33.09	23.4097	9.8684	0.2331	0.1302
	0.41	0.31	34.94	25.3081	9.8277	0.2359	0.1854
	0.4369	0.3065	37.9	28.0368	10.0701	0.2424	0.2645

Table 2. CIE color coordinates, cone contrast (the difference between the cone excitation of the stimulus and the cone excitation of background divided by the cone excitation of the background) and the contrast measured for each luminance level presented.

MLCM	CIE coordinates			Cone values			Contrast
	x	y	Y	L	M	S	$\frac{\sqrt{\left(\frac{\Delta L}{L}\right)^2+\left(\frac{\Delta M}{M}\right)^2+\left(\frac{\Delta S}{S}\right)^2}}{\sqrt{3}}$
	0.3023	0.3501	36.16	23.4569	12.9026	0.2717	0.2063
	0.3024	0.3502	42.53	27.5904	15.1741	0.3192	0.4184
	0.3025	0.3470	49.27	32.0006	17.5469	0.3766	0.6529
	0.3026	0.3457	56.68	36.8331	20.1689	0.4364	0.9060
	0.3028	0.3444	65.01	42.2725	23.1099	0.5040	1.1911
	0.3027	0.3430	72.74	47.3185	25.8422	0.5687	1.4587
	0.3031	0.3424	82.16	53.4753	29.1614	0.6438	1.7790
	0.3032	0.3414	91.91	59.8476	32.5992	0.7242	2.1146
	0.3034	0.3407	100.2	65.2729	35.5148	0.7923	2.3995
	0.3035	0.3400	111.6	72.7236	39.5340	0.8858	2.7911
Direct Estimation	x	y	Y	L	M	S	$\frac{\sqrt{\left(\frac{\Delta L}{L}\right)^2+\left(\frac{\Delta M}{M}\right)^2+\left(\frac{\Delta S}{S}\right)^2}}{\sqrt{3}}$
	0.3023	0.3501	36.16	23.4569	12.9026	0.2717	0.2063
	0.3024	0.3470	47.89	31.1018	17.0580	0.3662	0.6068
	0.3028	0.3546	61.52	40.0003	21.8716	0.4764	1.0727
	0.3031	0.3430	75.74	49.2862	26.8916	0.5915	1.5589
	0.3032	0.3414	92.1	59.9714	32.6666	0.7257	2.1211
	0.3035	0.3400	111.6	72.7236	39.5340	0.8858	2.7911

Stimuli were specified in the DKL color space [22-24]. This is a three-dimensional cone-opponent space based on the Smith and Pokorny (1975) cone fundamentals [25]. The first axis represents a luminance mechanism based on the sum of L and M cone excitations (L+M). The second axis represents the difference between the L and M cone excitations (L-M). Finally, the third axis defines lights that selectively modulate the S cones as L-M and L+M are constant along this axis. Hue direction is specified by the azimuth. Luminance is scaled between -1 and 1, where the value of 1 corresponds to the maximum of the monitor luminance and the value of -1 to the minimum. Chromatic strength ranges from 0 to 1 and refers to the maximum value along the axis that may be displayed on the monitor. Note that a value of 0 corresponds to the origin in DKL color space; increasing the distance from 0 in the equiluminant plane leads to increases in the perceived saturation of the stimulus.

The stimuli were defined with the gray background and red colors at azimuth of 0 deg. The saturation levels of the reddish colored stimulus varied from 0.1 to 1 along the L-M axis in DKL color space while the gray background was fixed at 0. In separate sessions, the red-gray checkerboard and the red square were replaced by a white-gray checkerboard and a white square. Here, the azimuth is fixed at 0 deg and the luminance elevations of the white color ranged from 0.1 to 1 along the L+M axis in the DKL color space.

The contrasts of the colored stimuli are presented in Table I and II. In both tables, the L, M and S cone contrasts were defined as the difference between the maximum cone excitation of the stimuli and the background and divided by the cone excitation of the background. Then, the stimulus contrast was calculated as $\frac{\sqrt{\left(\frac{\Delta L}{L}\right)^2+\left(\frac{\Delta M}{M}\right)^2+\left(\frac{\Delta S}{S}\right)^2}}{\sqrt{3}}$.

2.4 Procedure

Each observer completed the two experimental sessions on separate days. Observers were adapted to the grey background for 3 min at the beginning of each session. There was a practice session of 5 trials, followed by the experimental session, if the observer felt comfortable with the task; otherwise, additional practice trials were run. No feedback was provided during any part of the experiment.

Direct estimation task

Each stimulus was presented four times for each condition, tested in a random order. Each session consisted of 48 trials (2 patterns × 6 saturation levels × 4 repetitions). On each trial, a black fixation cross was presented in the center of the screen for 500 ms. At its offset, the stimulus appeared for 500 ms, followed by a blank screen. The participants were asked to rate the saturation level as a percentage indicating the chromatic sensation. Thus, the absence of chromatic sensation is indicated by 0% of saturation, and a maximal sensation corresponded to 100% of saturation. The subsequent trial was activated by pressing the appropriate button. A 1 s pause was interleaved between each trial.

Maximum Likelihood Conjoint Measurement task

In the MLCM experiments, 10 contrast levels and 2 stimulus patterns were used, generating a 2 × 10 grid of 20 stimuli. Figure 1 shows an example of the stimulus grid from which stimulus pairs were selected for patterns displayed along the L-M axis. On each trial, two different stimuli were chosen randomly from the 2 × 10 grid (see Figure 1); there are a total of (20×19)/2 = 190 non-identical pairs. A session consisted of the random presentation of all test pairs. It was repeated two times, yielding 380 trials for each observer.

Initially, a black fixation cross was presented in the center of the screen for 500 ms. When it disappeared, two stimuli were presented during 500 ms, followed by a blank screen. Observers were instructed to judge which pattern appeared more reddish or brighter, depending on the stimulus set. Responses were recorded as right or left button presses and initiated a 1 s pause before the initiation of the next trial. Overall, the MLCM sessions, including a rest between repetitions, lasted around 25 minutes while the DE task required about 15-20 minutes.

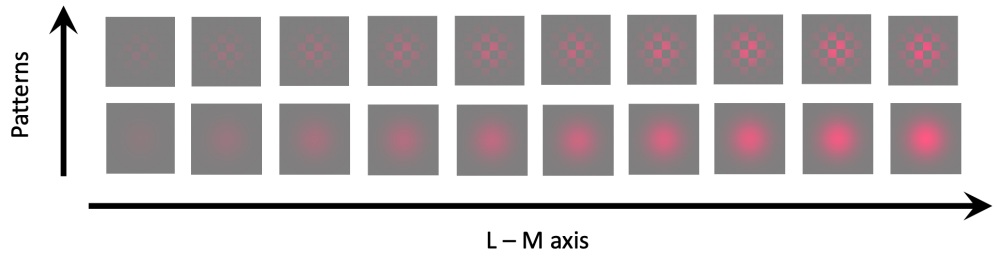

Fig. 1. Examples of stimulus set used for the Maximum Likelihood Conjoint Measurement experiment. Each row corresponds to a stimulus pattern, a checkerboard on the top and a square on the bottom. Each column represents different saturation levels displayed along the L-M axis.

2.5 Statistical Analyses

All statistical analyses were performed in the R statistical environment [26]. Data were plotted with functions from the **lattice** package [27]. Random effects analyses were performed using the *lmer* function in the **lme4** package [28].

3. Results

3.1 Saturation levels displayed along the L-M axis

Figure 2 shows each observer's mean saturation estimates for the DE task as a function of cone contrast for the square (white circles) and the checkerboard (black circles) stimuli. The column labels identify the observers; average functions are presented in the rightmost panels. The abscissa cone contrast levels of the uniform square were scaled to take into account that the space-averaged cone contrast levels of the red–gray checkerboard are one-half those of the uniform square of the same cone contrast levels [10]. The observers were ordered with respect to their estimations at the maximum contrast, and then their identifications were assigned so that Observer 1 gave the highest ratings and Observer 5 the lowest. The top row shows the results displayed with a linear abscissa while the bottom row displays the same data on a logarithmic abscissa. For both the chromatic checkerboard and uniform square, estimates increased monotonically with the cone contrast. The estimates for the chromatic checkerboard increased more steeply than those for the uniform square over the same cone contrast levels. On the log abscissa, the difference in steepness appears as a lateral shift of a roughly invariant shaped function. Informally, after the measurements were completed, observers reported the checkerboard to appear more saturated than the square at equal cone contrast, when presented side-by-side. These results replicate those found by Nunez et al. [20].

The data displayed individual variability in the range of estimated saturations and in the relative separation of the two curves. For example, the saturation estimated for the maximum contrast for Obs. 5 was 40% of that of Obs. 1. In addition, the two curves for Obs. 5 tend to overlap for low contrasts, whereas this does not occur for the other observers. Obs. 5 also tended to show more variable estimates.

(a)

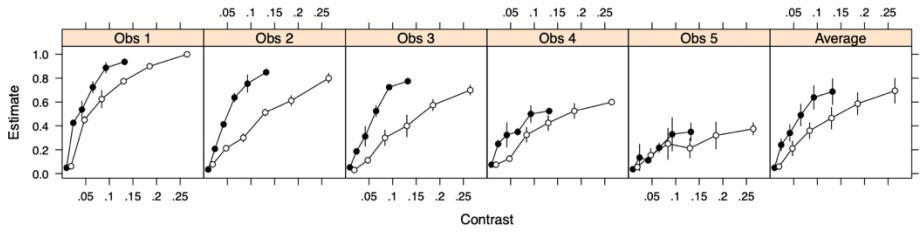

(b)

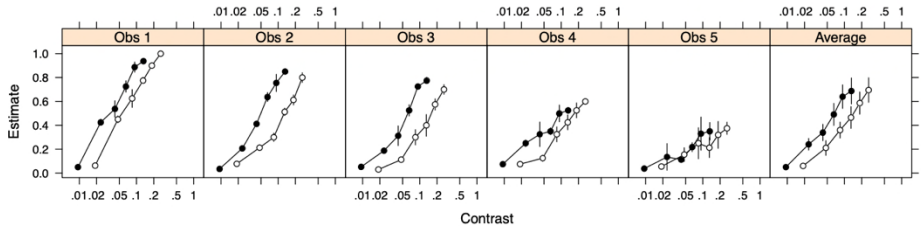

Fig. 2. Results obtained with a direct estimation procedure. Mean estimated scale presented as a function of cone contrast for the square (white circle) and the checkerboard (black circle) patterns displayed along the L-M axis. Data are presented with a (a) a linear scale and (b) a logarithmic scale. Error bars show +/- 1 SEM for estimates across the four repetitions.

For the MLCM procedure, the data were analyzed as a decision process within the framework of a signal detection model and fitted by maximum likelihood [5,6]. Perceptual contributions of each dimension were estimated using the software package MLCM [29] in the open-source software R [26].

Figure 3 shows the average estimated scales for each pattern obtained from fitting the additive model to the data of each of the 5 observers and the average functions. As in the previous figure, the abscissa values indicate the cone contrast values, with linearly spaced abscissa in Fig 3a and a logarithmically spaced abscissa in Fig. 3b. Filled circles represent the estimated checkerboard scale while open circles indicate the uniform square scale. The data follow the same qualitative pattern as in Figure 2, using the DE method. The contribution of the checkerboard pattern increases more steeply with cone contrast than the square pattern. On a logarithmic abscissa, curves of similar shape are simply translated along the abscissa. As the observers are ordered as in Fig. 2, the extent to which the two methods agree with respect to the response range can be evaluated. The response ranges of the estimated scales tend to follow those obtained using the DE method except for Obs. 5, who rather than showing the weakest responses as with DE, shows one of the strongest responses with MLCM.

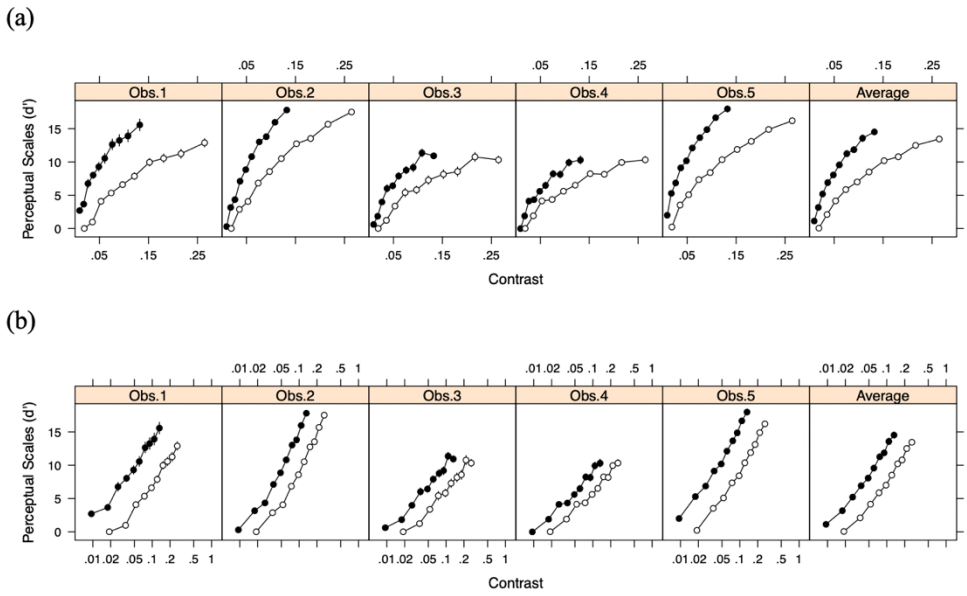

Fig. 3. Estimated scale obtained with MLCM procedure. Average estimates for the square (white circle) and the checkerboard (black circle) patterns displayed along the L-M axis as a function of cone contrast for five observers. Data are presented with a (a) a linear scale and (b) a logarithmic scale. Error bars show +/- 1 SEM for estimates across the two sessions.

3.2 Luminance levels displayed along the L+M axis

Results of the DE task for five observers are displayed in Figure 4 along with the average curves and are presented as a function of cone contrast for the checkerboard (black circles) and for the square (white circles). Results for both patterns show a qualitatively similar pattern as that along the L-M axis with estimates increasing monotonically with contrast, except for Obs. 7. The estimated contrast of the checkerboard was higher than that of the uniform square and on

the logarithmic abscissa, the curves appear to differ only by a lateral translation. There are individual differences in the range of estimates that the observers used. Obs. 7 generated less consistent estimates as indicated by the larger error bars and the estimates varied non-monotonically with contrast. Again, the ordering in the figures is with respect to maximum estimates along the scales in order to facilitate comparison with the MLCM measures.

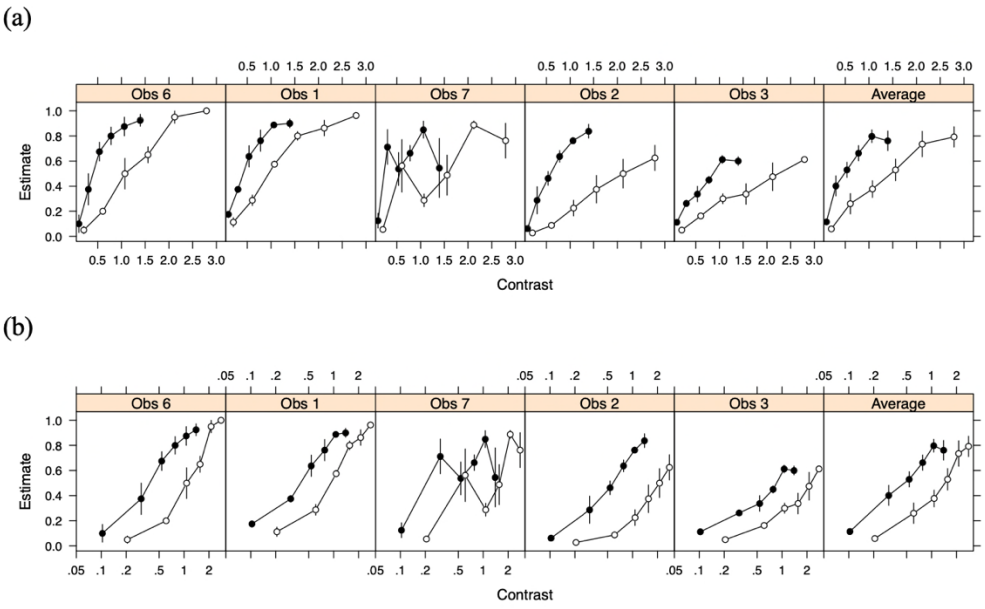

Fig. 4. Estimated scale obtained with direct estimation procedure. Mean estimated scale presented as a function of cone contrast for the square (white circle) and the checkerboard (black circle) patterns displayed along the L+M axis across all observers. Data are presented with a (a) a linear scale and (b) a logarithmic scale. Error bars show +/- 1 SEM for estimates across the four repetitions.

Scales estimated from the MLCM procedure are displayed in Figure 5, using the same format as the previous figures. Results show the average estimated scales under the additive model for each observer. Filled circles indicate the estimated checkerboard scales and open symbols the square scales. The values on the abscissa indicate the 10 cone contrast values for each dimension as displayed along the L+M axis in the DKL color space. The MLCM results agree qualitatively with those from the DE method in the relative forms and spacing of the two curves. The range of responses for DE and MLCM agree across methods except for Obs. 6, whose MLCM responses are relatively smaller compared to those for DE. Also, the response curves of Obs. 7 are more orderly for MLCM than for DE.

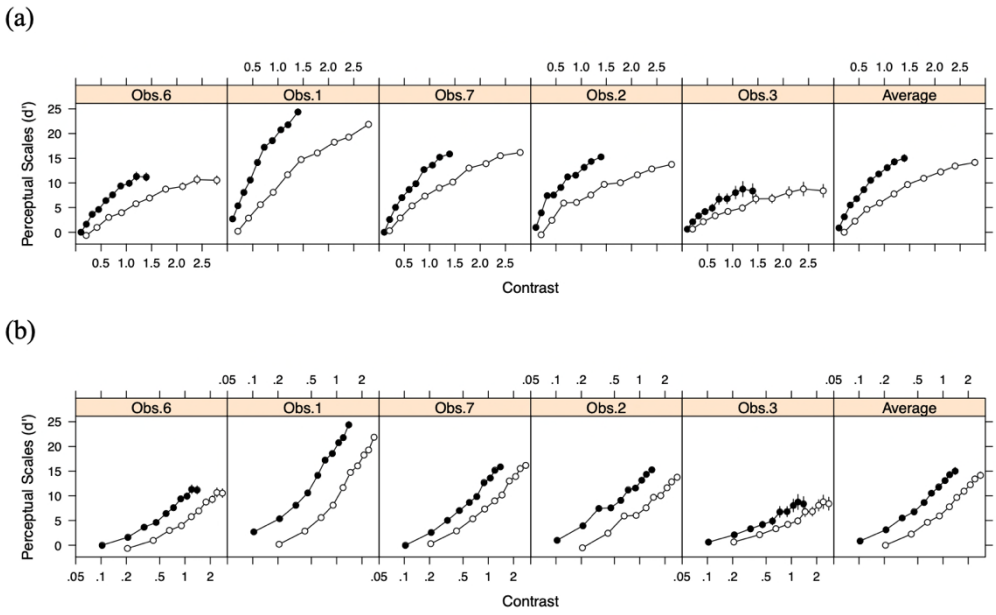

Fig. 5. Estimated scale obtained with MLCM procedure. Additive model average estimates for the square (white circle) and the checkerboard (black circle) luminance patterns as a function of cone contrast for five observers. Data are presented with a (a) a linear scale and (b) a logarithmic scale. Error bars show +/- 1 SEM for estimates across the two sessions.

3.3 Comparison between Direct Estimation and MLCM methods.

Since the DE and MLCM methods yield response curves that are on different scales, we compared variability using the coefficient of variation (CV), defined as the standard deviation divided by the mean and that provides a measure of relative variability. Figure 6 compares the CV across method for each pattern and color axis, using box-and-whisker plots. The medians (black points) are similar across methods and the interquartile ranges (grey boxes) overlap, suggesting that there is little difference in variability between the two methods. This is confirmed by fitting the data with a linear model with contrasts chosen to compare the means within each panel of Figure 6 (L+M/Check: $t(278) = 0.422$, $p = 0.673$; L+M/Square: $t(278) = 0.985$, $p = 0.325$; L-M/Check: $t(278) = 0.779$; $p = 0.437$; L-M/Square: $t(278) = 1.213$, $p = 0.226$). Because all of the explanatory variables are factors, this is technically an analysis of variance, but we only concentrate on the pre-planned contrasts of interest here, which are distributed as t-statistics. None of the contrasts were significant so that corrections for multiple tests would not affect the (non-)significance of the results. These plots, however, collapse the data over subject and contrast level.

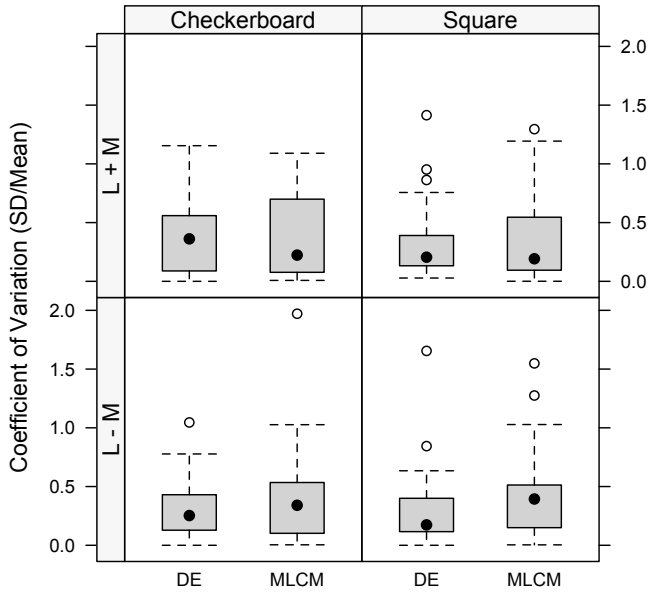

Fig. 6: Comparison of DE and MLCM estimated with the coefficient of variation (CV) for the checkerboard (left side) and the square (right side) displayed along the L+M (top row) and L-M axes (bottom row) as a function of cone contrast. Filled symbols represent the medians, and the grey boxes indicate the interquartile ranges (IQR). The whiskers are defined to extend to the most extreme data points within 1.5 times the IQR from the box. Any data points outside the whiskers are plotted as unfilled symbols.

Figure 7 shows the CVs for each individual plotted as a function of contrast for both methods for both patterns and for both axes in color space. Within observer, the CV appears to be more stable for the MLCM than for the DE method. The MLCM values do not appear to depend systematically on contrast, stimulus or color axis except for a few observers along the L - M axis, who show a jump at the lowest contrast. High variability for small means (e.g., at low contrasts) will inflate the CV. For some observers, the DE values fluctuate unsystematically with contrast. There appears to be greater variability of the CV across observers for MLCM than DE, however. This is supported by a random effects analysis for each method. The within observer variance for DE accounts for 90% of the variance while only 71% for MLCM. The across observer variance for MLCM is 4.7 times greater than that for DE.

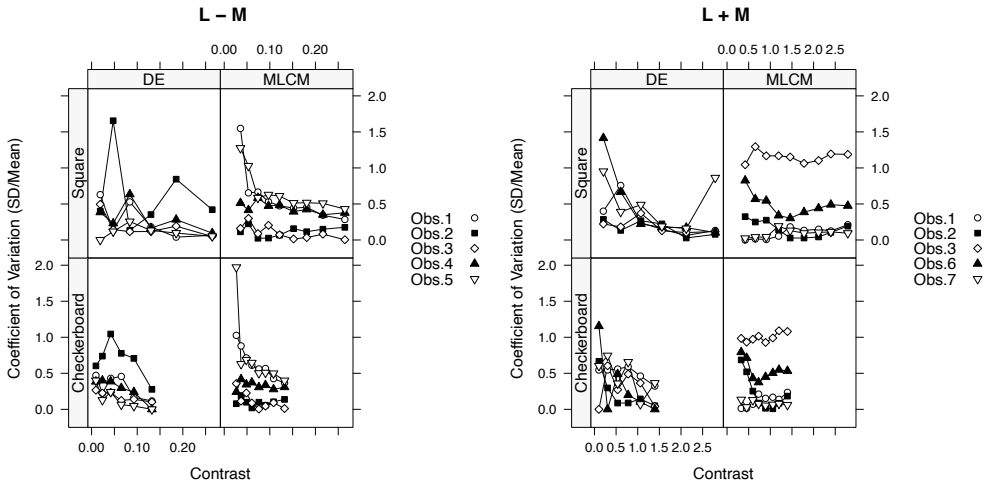

Fig. 7. The CVs for each observer plotted as a function of cone contrast for each procedure and pattern. Panels on the left side display the results for the L-M axis, and panels on the right side indicate the results for the L+M axis. Symbols assigned to each observer are indicated in the legends.

4. Discussion

DE methods have been widely used to measure color appearance as they are relatively fast and simple to implement [30]. However, the task has been criticized as not necessarily measuring color appearance alone but also reflecting the observer's perception of numbers, especially for naïve observers. The qualitative similarity in the shapes of the functions obtained for the two methods provides some validation of the DE approach for color scaling. In most cases, individual differences in ordinal strength of the estimated appearance correlate between methods, but some glaring exceptions occur. It is possible that the variability of some of the observers for the DE results reflects uncertainties in the task rather than aspects of color appearance *per se*. Such uncertainties might be reduced by presenting observers at the beginning of a DE session with examples of the highest and lowest contrasts and indicating that these should receive the most extreme ratings. This procedure, however, would force the functions for different patterns to attain the same maximum value, even if the actual appearances are not equal. The MLCM procedure is based on a more intuitive response that requires the observer only make an ordinal judgment, i.e., to choose which of a pair of stimuli appears more reddish or brighter. The appearance scale is then derived from a model of the observer's decision process using a maximum likelihood criterion [6].

Here, we repeated the DE task 4 times at 6 contrast levels which required 48 judgments. Repeating the MLCM task twice using 10 contrasts required 3.5 times as many trials. Nevertheless, the MLCM sessions on average only lasted about 5 minutes longer than those using DE. Thus, given that the DE sessions lasted about 20 minutes, it might be expected to require at least an hour to acquire as many trials from DE as from the MLCM task.

In general, the two tasks yielded similar results. As previously reported using DE for stimuli modulated along the L-M axis [20], the contribution of the checkerboard pattern increases more steeply with cone contrast than the uniform pattern. We report, here, the same behavior for stimuli modulated along the L+M axis. We found comparable results along both color axes using MLCM, thereby recommending it as an alternative procedure that is more intuitive for naïve observers.

When the results are plotted as a function of log contrast, the scales for the two patterns appear invariant in shape except for a lateral translation along the abscissa. This behavior is consistent with a single mechanism that is less sensitive to uniform fields than checkerboard stimuli. Evidence for multiple mechanisms is supported by results from VEP studies [11,20,21,31] that show, for example, different contrast dependencies of the response latency across patterns. The similar behavior along the L+M axis would be expected given the low-frequency fall-off of the luminance contrast sensitivity function and the evidence for multiple spatially tuned channels in the visual system [32]. These results are also supported by recent evidence indicating separate mechanisms for luminance coding of surface and patterns in cortical area V1 [33,34].

There was a trend across most observers for scale strengths to agree across methods, i.e., observers with high ratings at maximum contrast using DE also displayed strong perceptual responses at maximum contrast as estimated by MLCM. There were some notable exceptions, however, in which low response on DE was matched with high response on MLCM (Obs 5 along the L-M axis, Figs 2 and 3) and vice versa (Obs 6 along the L+M axis, Figs 4 and 5). We suspect that such differences reflect individual biases in how these observers assign numbers to perceptual events.

There were also differences in within-subject variation between methods. On the one hand, DE methods were relatively more variable within observer, perhaps reflecting observer uncertainty in assigning ratings. On the other hand, MLCM scales showed greater relative variability across observers. Given the lower within subject variability of MLCM, we believe these across observer differences are indicative of actual individual differences in the appearance of the stimuli, i.e., individual differences in how they are perceived. Perhaps, additional practice sessions prior to data collection would further minimize variability as well as differences between methods.

In conclusion, modeling of decisions based on simple ordinal judgments of pairs of stimuli largely reproduces the results from direct estimation of perceptual attributes of individual stimuli. Occasional differences between the two methods may reflect level of observer practice or biases in the assignment of numbers to perceptual magnitudes.

Funding. K. Knoblauch was supported by LABEX CORTEX (ANR-11-LABX-0042) of Université de Lyon (ANR-11-IDEX- 0007) and (ANR-19-CE37-0000, DUAL_STREAMS) operated by the French National Research Agency.

Acknowledgments. We thank John S. Werner for critical comments of an earlier draft of the manuscript.

Disclosures. The authors declare no conflicts of interest.

Data availability. Data underlying the results presented in this paper are not publicly available at this time but may be obtained from the authors upon reasonable request.

References

1. L.M. Hurvich, and D. Jameson, "Some quantitative aspects of an opponent-colors theory. II. Brightness, saturation, and hue in normal and dichromatic vision," J. Opt. Soc. Am. **45**, 602-616 (1955).
2. J.S. Werner, and B.R. Wooten, "Opponent chromatic mechanisms: Relation to photopigments and hue naming," J. Opt. Soc. Am. **69**, 422–434 (1979).
3. J. Gordon, I. Abramov, and H. Chan, "Describing color appearance: hue and saturation scaling," Percept. Psychophys. **56**, 27-41 (1994).
4. C.N. Matera, K.J. Emery, V.J. Volbrecht, K. Vermuri, P. Kay, and M.A. Webster, "Comparison of two method of hue scaling," J. Opt. Soc. Am. A **37**(4), A44-A54 (2020).
5. Y.X. Ho, M.S. Landy, and L.T. Maloney, "Conjoint measurement of gloss and surface texture," Psychol. Sci. **19**, 196–204 (2008).
6. K. Knoblauch, and L.T. Maloney, *Modeling Psychophysical Data in R* (Springer, 2012).
7. D.M. Green, and J.A. Swets, *Signal Detection Theory and Psychophysics* (Wiley, 1966).

8. L.T. Maloney, and K. Knoblauch, “Measuring and modeling visual appearance,” Annu. Rev. Vis. Sci. **6**, 519-537 **(**2020**)**.
9. G. Aguilar, and M. Maertens, “Toward reliable measurements of perceptual scales in multiple contexts,” J. Vis. **20**, 4:19 **(**2020**)**.
10. H.C. Sun, D. St-Amand, C.L. Baker, and F.A.A. Kingdom, “Visual perception of texture regularity: Conjoint measurements and a wavelet response-distribution model,” PLoS Comp. Biol. **17**, 10:e1008802 **(**2021**)**.
11. R.M. Shapley, V. Nunez, and J. Gordon., “Cortical double-opponent cells and human color perception,” Curr. Opin. Behav. Sci. **30**, 1-7 (2019).
12. E.N., Johnson, M.J. Hawken, and R. Shapley, “The spatial transformation of color in the primary visual cortex of the macaque monkey,” Nature Neurosci. **4**, 409-416 (2001).
13. P. Lennie, J. Krauskopf, and G. Sclar, “Chromatic mechanisms in striate cortex of macaque,” J. Neurosci. **10**, 649-669 (1990).
14. M.S., Livingstone, and D.H. Hubel, “Anatomy and physiology of a color system in the primate visual cortex,” J. Neurosci. **4**, 309-356 (1984).
15. R. Shapley, and M.J. Hawken, “Color in the cortex: single- and double-opponent cells,” Vision Res. **51**, 701-717 (2011).
16. R.M. Shapley, M.J. Hawken, and E.B. Johnson, “Color in primary visual cortex,” in *The New Visual Neurosciences*, J.S. Werner, and L.M. Chalupa, eds. (MIT Press, 2014), pp. 569–586.
17. D. Schluppeck, and S.A. Engel, “Color opponent neurons in V1: A review and model reconciling results from imaging and single-unit recording,” J. Vis. **2**, 480-492 (2002).
18. L.G. Thorell, R.L. De Valois, and D.G. Albrecht, “Spatial mapping of monkey V1 cells with pure color and luminance stimuli,” Vision Res. **24**, 751-769 (1984).
19. E.N. Johnson, M.J. Hawken, and R. Shapley, “The orientation selectivity of color-responsive neurons in macaque V1,” J. Neurosci. **28**, 8096-8106 (2008).
20. V. Nunez, R. Shapley, and J. Gordon, “Cortical double-opponent cells in color perception: Perceptual scaling and chromatic visual evoked potentials,” i-Perception **9**, 1-16 (2018).
21. V. Nunez, J. Gordon, and R.M. Shapley, “A multiplicity of color-responsive cortical mechanisms revealed by the dynamics of cVEPs,” Vision Res. **188**, 234-245 **(**2021**)**.
22. D.I. MacLeod, and R.M. Boynton, “Chromaticity diagram showing cone excitation by stimuli of equal luminance,” J. Opt. Soc. Am. **69**, 1183-1186 (1979).
23. J. Krauskopf, D.R. Williams, and D.W. Heeley, “Cardinal directions of color space,” Vision Res. **22**, 1123-1131 (1982).
24. A.M. Derrington, J. Krauskopf, and P. Lennie, “Chromatic mechanisms in lateral geniculate nucleus of macaque,” J. Physiol. (Lond.) **357**, 241-265 (1984).
25. V.C. Smith, and J. Pokorny, “Spectral sensitivity of the foveal cone photopigments between 400 and 500 nm,” Vision Res. **15**(2), 161-171 (1975).
26. R Core Team, *R: A language and environment for statistical computing. Vienna, Austria: R Foundation for Statistical Computing* (2021). URL https://www.R-project.org/.
27. D. Sarkar, *Lattice: Multivariate Data Visualization with R* (Springer, 2008).
28. D. Bates, M. Maechler, B. Bolker, and S. Walker, “Fitting Linear Mixed-Effects Models Using lme4,” Journal of Statistical Software, **67**(1), 1-48 (2015).
29. K. Knoblauch, and L.T. Maloney, and G. Aguilar, *MLCM: Maximum Likelihood Conjoint Measurement. R package version 0.4.3* (2019). https://CRAN.R-project.org/package=MLCM
30. I. Abramov, and J. Gordon, “Color appearance: on seeing red, or yellow, or green, or blue,” Annu. Rev. Psychol. **45**, 451-85 **(**1994**)**.
31. V. Nunez, R. Shapley, and J. Gordon, “Signals from single-opponent cortical cells in the human cVEP,” J. Neurosci. **42**(21), 4380-4393 (2022).
32. F.W. Campbell, and J.G. Robson, “Application of Fourier analysis to the visibility of gratings,” J. Physiol. (Lond.) **197**, 3:551-66 **(**1968**)**.
33. Y. Yang, T. Wang, Y. Li, W. Dai, G. Yang, C. Han, Y. Wu, and D. Xing, “Coding strategy for surface luminance switches in the primary visual cortex of the awake monkey,” Nature Commu. **13**, 1:286 (2022).
34. G. Zurawel, I. Ayzenshtat, S. Zweig, R. Shapley, and H. Slovin, “A contrast and surface code explains complex responses to black and white stimuli in V1,” J. Neurosci. **34**, 43:14388-402 (2014).